Realizing Anapole-FP Cavity Strong Coupling in a Silicon-Based Metasurface Hybrid System

Wei Liu, Yu Tang, Zhengqi Liu, Junjie Li, Yang Cheng, and Guiqiang Liu

***Abstract*—Manipulation of light-matter interactions has great potential applications in optical modulators and optical switches. However, the strong coupling of anapole-cavity modes has not been involved yet. Here, we firstly propose a simple Si-based metasurface hybrid system to realize tunable strong coupling of anapole-Fabry-Pérot (FP) cavity via inserting a Si square nanocubes metasurface inside an FP nanocavity. A remarkable spectral splitting behavior is achieved with large Rabi splitting of 192 meV due to the strong resonant coupling between the anapole and FP cavity modes. The induced two hybrid energy states are respectively dominated by the anapole mode and cavity mode and can be tuned by the length of FP nanocavity and the thickness of SiO_2 spacer, respectively. This Si-based metasurface system opens an avenue for designing opto-electronic devices that can manipulate light-matter interactions at nanoscales.**

***Index Terms*—Light-matter interactions, strong coupling, rabi splitting.**

I. Introduction

MANIPULATION of light-matter interactions has attracted a lot of attention in recent years due to the wide applications in directional light emission [1], all-optical switching [2] and quantum information processing [3], etc. An especially interesting regime (i.e., strong coupling) in light-matter interactions is achieved when the rate of coherent energy exchange between individual systems becomes faster than any of their intrinsic dissipation rates [4], [5]. New hybrid states can be thus generated with half-light and half-matter features, accompanied by prominent feature-mode splitting in the optical spectrum, i.e., Rabi splitting [6], [7]. Strong coupling behaviors in hybrid systems can also be used to explore some fundamental physics problems such as Bose-Einstein condensation [8] and super fluid related phenomena [9] and are very useful in many exciting fields, e.g., single photon transistors [10], polariton nanolasers [11] and photonic quantum devices [12].

High-index dielectric nanostructures have recently gained considerable attention for studying and boosting light-matter interactions, e.g., improving nonlinear conversion [13], enhancing harmonic generation [14] and intensifying local fields [15] due to the low-cost manufacturing, excellent compatibility and pronounced low-loss properties [16], [17]. A new nonradiate electromagnetic mode, i.e., anapole mode, was recently discovered in high-index nanoparticles [18], [19], which originates from the destructive interference between the electrical dipole (ED) and toroidal dipole (TD) moments. The anapole mode can be used to suppress total scattered field, enhance near field energy [20], and realize ideal magnetic dipole (MD) [21], and improve quality (Q)-factors [22]. Recently, hybrid energy states have also been obtained via the strong coupling behaviors in the anapole-exciton, anapole-plasmon and anapole-exciton-plasmon hybrid systems consisting of silicon (Si) nanoparticles and various hybrid systems including Si nanodisk-bulk WS_2 [23], molecular J-aggregate rings [24], dielectric-metal nanostructures [25], [26] and Ag nanodisk-monolayer WSe_2 [27]. Large Rabi splitting values of 120–275 meV were achieved in these systems. However, it is still a hotspot to design a hybrid system with strong coupling of anapole and other modes to artificially manipulate light-matter interactions at nanoscales.

Fabry-Pérot (FP) microcavities are capable of enhancing the localized field energy by coupling external light into an ultrasmall volume on the basis of multiple round-trip reflection and flexibly tunable FP cavity modes [28]. Very recently, innovative hybrid systems were built to study the strong coupling behaviors via integrating the FP microcavities with novel nanostructures. For instance, Li et al. presented the strong coupling of single-exciton with localized surface plasmons by placing a Au@Ag NR/J-aggregate hybrid on a leaky FP cavity and improved the success rate of strong coupling by 79% [29]. Xie et al. reported the strong coupling of photonic bound states in the continuum (BICs)-cavity modes by embedding an Si pillar pairs metasurface into a low-Q FP microcavity [30] and the cavity-assisted strong coupling of quasi-BICs-excitons by replacing the Si pillar pairs metasurface with the bulk WS_2 pillar pairs metasurface [31]. Baranov et al. demonstrated the strong plasmon-microcavity coupling by inserting a plasmonic nanorod array into an FP microcavity [32]. These have laid and excellent foundation for the research of strong coupling based on the FP cavity mode. However, to the best of our knowledge, the strong coupling of anapole-FP cavity modes has not been involved yet.

In this work, for the first time, we propose a simple hybrid structure consisting of a Si square nanocubes metasurface and a common FP nanocavity to firstly realize strong coupling of anapole mode and FP cavity mode. A large Rabi splitting value

Manuscript received 3 September 2023; revised 5 October 2023; accepted 9 October 2023. Date of publication 13 October 2023; date of current version 24 October 2023. This work was supported in part by the National Natural Science Foundation of China under Grants 62275112, 51761015, and 11564017 and in part by the Natural Science Foundation of Jiangxi Province under Grants JXSQ2019201058 and 20232ACB201009. *(Wei Liu and Yu Tang are co-first authors.) (Corresponding author: Guiqiang Liu.)*

The authors are with the College of Physics and Communication Electronics, Jiangxi Normal University, Nanchang, Jiangxi 330022, China (e-mail: 202140100607@jxnu.edu.cn; 13247705669@163.com; zliu@jxnu.edu.cn; 202240100601@jxnu.edu.cn; chengyang688@jxnu.edu.cn; liugq@jxnu.edu.cn).

Digital Object Identifier 10.1109/JPHOT.2023.3324204

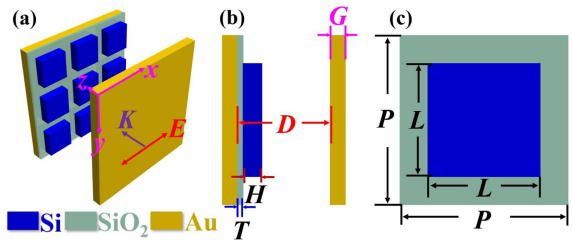

Fig. 1. Schematics of Si-based metasurface hybrid system, (a) cross-section (b) and unit cell (c).

of 192 meV is obtained due to the strong of anapole-FP cavity mode coupling, which induces the generation of two new hybrid energy states, i.e., upper and lower branches (UB and LB states). The UB and LB states are respectively dominated by the anapole mode and cavity mode and can be flexibly modified by the thickness of the SiO_2 spacer and the length of the FP nanocavity. These open an avenue for the design of optoelectronic devices to manipulate light-matter interactions at nanoscales.

II. Design and Method

The proposed Si-based metasurface hybrid system is illustrated in Fig. 1(a). It consists of a 2D rectangular periodic array of Si square nanocubes placed in an FP nanocavity formed by two Au mirrors with an ultrathin layer of SiO_2 as a spacer. Fig. 1(b) shows the cross-sectional view of the metasurface hybrid system in the y-z plane. The distance between the two Au mirrors, i.e., the cavity length is marked with D. The thickness values of Au mirrors, Si nanoblocks and SiO_2 spacer are denoted as G, H and T, respectively. Fig. 1(c) displays the unit cell with the period $P = 450$ nm. The side length of Si square nanoblocks is marked with L. Here, $D = 280$ nm, $G = 40$ nm, $H = 40$ nm, $L = 340$ nm, and $T = 15$ nm, except where otherwise stated. The optical responses are calculated by the three-dimensional finite-difference time-domain (FDTD) method. An x-polarized plane wave is incident on the metasurface hybrid system along z direction with the wavelength ranging from 600 to 800 nm. Periodic boundary conditions are used in the x-y plane and perfectly matched layer conditions are used in the z direction. The grid size is 2 nm. The permittivity of Si is taken from Refs. [33], [34] The permittivity of Au is extracted from the Drude model expressed by $\varepsilon = \varepsilon_\infty - (\omega^2{}_p/\omega(\omega + i\gamma))$ with $\varepsilon_\infty = 9.07$ and $\omega_p = 1.35 \times 10^{16}$ rad/sec [33], [35]. The index of SiO_2 is 1.46. The Si-based metasurface hybrid system is placed in air with refractive index of 1.0.

III. Results and Discussions

Fig. 2(a) shows the absorption spectra of the rectangular periodic array of Si nanoblocks with different L values ($H = 40$ nm). A prominent resonance peak is observed with an obvious redshift when L increases from 300 nm to 380 nm. For the pure FP nanocavity with $D = 280$ nm and $G = 40$ nm, a distinct absorption peak is also found at 681 nm (Fig. 2(b)), overlapping with that of the Si nanoblocks with $L = 340$ nm in Fig. 2(a). By integrating the Si nanoblock periodic array, the FP nanocavity

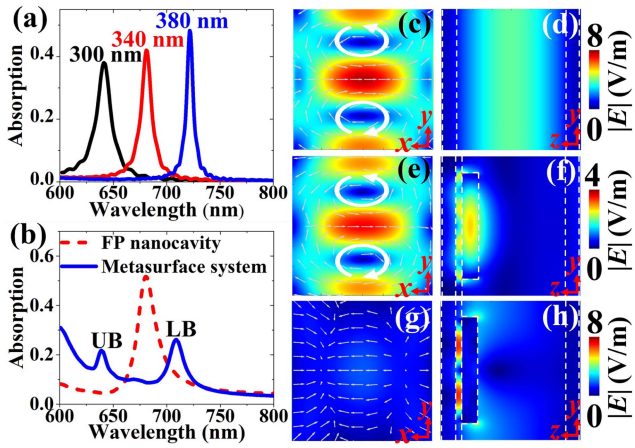

Fig. 2. Absorption spectra of (a) Si nanoblock array and (b) FP nanocavity and metasurface hybrid system. Electric field distributions of (c) Si nanoblock array, (d) FP nanocavity and metasurface hybrid system at (e), (f) UB and (g), (h) LB states. Arrows: directions of electric field energy flow.

and the spacer layer of SiO_2 ($T = 15$ nm) together, two obvious absorption peaks at 639 nm and 709 nm, namely UB and LB states, are achieved as shown in Fig. 2(b).

In order to understand the physical mechanisms of the phenomena observed above, corresponding electric field distributions are calculated. Fig. 2(c) shows the electric field distribution of Si nanoblocks with $L = 340$ nm for the absorption peak at 681 nm as observed in Fig. 2(a). Two reverse circular displacement currents are clearly observed in the x-y plane with energy confined inside the Si nanoblocks, similar to that reported in [36], demonstrating the excitation of anapole state. In Fig. 2(d), concentrated electric filed energy is found in the center of the pure FP nanocavity, verifying the appearance of FP cavity mode. Fig. 2(e) and (f) present the electric field distributions for the UB state in the metasurface hybrid system in the x-y and y-z planes, respectively. The same electric field distribution pattern of UB state as that observed in Fig. 2(c) indicates that this UB state is dominated by the anapole state of Si nanoblocks. The electric filed energy for the LB state in the metasurface hybrid system is not concentrated in the Si nanoblocks (Fig. 2(g)) but in the SiO_2 spacer (Fig. 2(h)) and is greatly enhanced compared to that of the pure FP nanocavity, implying the domination role of FP cavity mode and the field enhancement role of anapole mode. Therefore, it can be concluded that the anapole modes can serve as a potential platform to manipulate and enhance the light-matter interactions at nanoscales.

In order to further understand the strong anapole-cavity coupling in the metasurface hybrid system, related multipolar scattering powers are calculated by multipolar expansion methods [37], [38]. The scattering power curves of ED, MD, TD, electric quadrupole (EQ) and magnetic quadrupole (MQ) of Si nanoblocks array with $L = 340$ nm are shown in Fig. 3(a). The intersect found at 681 nm in the curves of ED and TD moments indicates the ED moment destructively interfering with the TD moment in the far field, i.e., the excitation of anapole mode [36]. The scattering power curves of multipolar components of the pure FP nanocavity are given in Fig. 3(b). Obviously, the

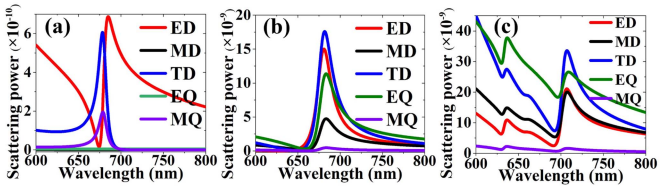

Fig. 3. Scattering powers of multipole moments in (a) Si nanoblocks array, (b) FP nanocavity and (c) metasurface hybrid system.

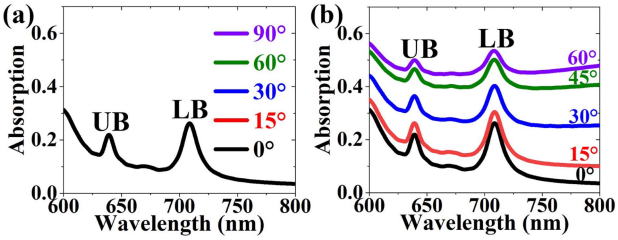

Fig. 4. Absorption spectra of Si-based metasurface hybrid system at different polarization (a) and incident angles (b).

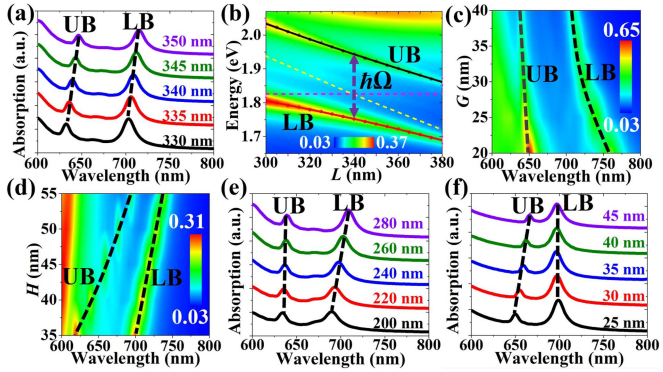

Fig. 5. (a) Absorption spectrum of the metasurface hybrid system with different L value. (b) Dispersion curve of the metasurface system obtained by metasurface oscillator model (solid lines) and fitted absorption (spheres) as a function of L. Red and yellow dashed lines respectively represent the FP nanocavity and Si nanoblocks energies. Absorption contour maps of the metasurface system with (c) different Au mirror thickness G and (d) different Si nanoblocks height H. Absorption spectra of the metasurface hybrid system with (e) different nanocavity length D and (f) different SiO_2 spacer thickness T.

scattering power is dominated by the ED and TD components but without an intersection at 681 nm, again demonstrating the generation of FP cavity mode [30]. Fig. 3(c) shows the scattering power curves of multipolar components of the metasurface hybrid system. For the LB state, the scattering power of different electromagnetic components is essentially the same as the FP cavity mode, indicating that the LB state mainly derives from the FP cavity mode. For the UB state, it no longer remains the same pattern as that of the original anapole mode due to the strong influence of FP cavity mode via the strong coupling of anapole-FP cavity mode.

To give a deep insight into the coupling property in the hybrid system, Fig. 4(a) and (b) respectively shows the absorption spectra of Si-based metasurface hybrid system at different polarization and incident angles. It can be found the absorption spectrum of Si-based metasurface system is almost unchanged with the polarization angle increasing from 0 to 90° (from x-polarized to y-polarized light), indicating the polarization independence of Rabi splitting (Fig. 4(a)). The insensitivity of polarization can be ascribed to the symmetric metasurface used in this system, which can be used to exploit the strong coupling optical devices that are not affected by the polarization light. The absorption peaks gradually disappear with the increase of incident angle but the positions of the UB and LB states are almost invariable (Fig. 4(b)). The decline in intensity mainly results from the weakened strong coupling of anapole and FP cavity modes.

Fig. 5(a) displays the absorption spectrum of the metasurface hybrid system with different L value. Black dash lines indicate the peak positions of LB and UB states. As analyzed in Fig. 2(a), the resonant position of the anapole mode is closely related to the dimension of Si nanocubes. When L increases, the resonant position of anapole mode would move to the long wavelength region, which leads to the distinct red-shifts of both UB and LB states via the strong coupling of anapole-FP cavity mode. Fig. 5(b) shows the corresponding dispersion curves as a function of L. The "energy" axis represents the wavelength of incident light. The values of UB and LB states are extracted from the absorption spectra shown in Fig. 5(a). A typical anti-crossing behavior, i.e., Rabi splitting, is observed, indicating that the strong coupling between the anapole mode and FP cavity mode appeared in this system. The coupling strength and the Rabi splitting behavior can be analyzed by the coupled oscillator model [39]:

$$\begin{pmatrix} E_A - i\Gamma_A/2 & g_{AC} \\ g_{AC} & E_C - i\Gamma_C/2 \end{pmatrix} \begin{pmatrix} \alpha \\ \beta \end{pmatrix} = E \begin{pmatrix} \alpha \\ \beta \end{pmatrix} \quad (1)$$

where E_A and E_C represent the resonance energies of uncoupled anapole and cavity modes, respectively. g_{AC} is the coupling strength. Γ_A and Γ_C are the resonance linewidths of the uncoupled anapole and cavity modes, respectively. α and β are the components of the eigenvectors, satisfying $|\alpha|^2 + |\beta|^2 = 1$. By diagonalizing (1), eigenvalues $E_\pm$ can be calculated from

$$E_\pm = \frac{1}{2}(E_A + E_C) - \frac{i}{4}(\Gamma_A + \Gamma_C) \pm \frac{1}{2}\sqrt{4g_{AC}^2 + \left[\delta - \frac{i}{2}(\Gamma_A - \Gamma_C)\right]^2} \quad (2)$$

When the detuning energy between the anapole and the cavity modes ($\delta = E_A - E_C$) is zero, i.e., $\delta = 0$, the value of Rabi splitting can be expressed by [7]

$$\hbar\Omega = \sqrt{4g_{AC}^2 - (\Gamma_A - \Gamma_C)^2/4} \quad (3)$$

Here, absorption linewidths derive from Fig. 2(a) and (b) with $\Gamma_A = 56$ meV and $\Gamma_C = 106$ meV, respectively. As shown in Fig. 5(b), the anti-crossing behavior between LB and UB states occurs at $\delta = 0$ with the Rabi splitting value high to $\hbar\Omega = 192$ meV. The coupling strength between the anapole and FP cavity modes can be obtained by (3) with $g_{AC} = 96$ meV. The strong coupling criterion $\hbar\Omega > (\Gamma_A + \Gamma_C)/2$ is fully satisfied [40], which confirms the existence of strong coupling between the anapole mode and FP cavity mode.

In Fig. 5(c), the LB and UB states both show blue-shifts and the LB state moves more quickly than the UB when the thickness G of Au mirror increases from 20 nm to 40 nm. This indicates

TABLE I
COUPLING RELATED TO NANOSTRUCTURE LITERATURE COMPARISON

Ref.	Hybrid structure	Coupling type	Rabi splitting (meV)
[6]	Si_3N_4 nanodisks metasurface –bulk WS_2	TD-exciton	65
[23]	Si nanodisk-bulk WS_2	anapole-exciton	151
[24]	Si nanodisk-molecular J-aggregates ring	anapole-exciton	161
[25]	Si nanodisk-Au nanostrip dimer	anapole-plasmon	120
[26]	Si nanoblock-Ag nanodisk	anapole-plasmon	275
[27]	Si nanodisk-Ag nanodisk-monolayer W Se_2	anapole-plasmon-exciton	159
[30]	Si pillar pairs metasurface-FP cavity	quasi-BIC-FP cavity	220
[31]	Bulk WS_2 pillar pairs metasurface-FP cavity	quasi-BIC-exciton-FP cavity	464
Our work	Si nanoblocks metasurface-FP cavity	anapole-FP cavity	192

that the increased Au thickness can be used to adjust the FP cavity resonance and produces a stronger effect on the LB state. In Fig. 5(d), it can be clearly seen that the LB and UB states both have obvious red-shifts with increasing the height H of Si nanocubes in the range of 35–55 nm due to an increase of the effective refractive index of the FP cavity [30]. Contrarily, the UB state moves more significantly as compared to the LB state due to the main contributor of the anapole mode to the UB state. Therefore, it can be concluded that the LB and UB states are respectively dominated by the FP cavity mode and anapole mode in this hybrid system.

Fig. 5(e) displays the absorption spectrum of the metasurface hybrid system with the nanocavity length D increasing from 200 nm to 280 nm. The variation of D has almost no influence on the UB state but has an obvious effect on the LB state. The increased length of FP cavity can lead to the prominent red-shift of FP cavity mode [30], [31]. As a result, the red-shift of LB state occurs, again verifying the contribution of the FP cavity mode to the LB state. In Fig. 5(f), when the thickness T of the SiO_2 spacer increases from 25 nm to 45 nm, the LB state is almost invariable due to the slight variety in length of FP cavity. While for the UB state, it shifts to the longer wavelength region owing to the decreased coupling strength between the anapole mode and FP cavity mode, resulting in the decrease of Rabi splitting with T in the hybrid system. These indicate that the UB and LB states in the anapole-cavity metasurface hybrid system can be artificially adjusted by the thickness of SiO_2 spacer and the length of FP nanocavity.

Table I shows a brief comparison of coupling related reports and Rabi splitting values (these results are all obtained via theoretical calculation) in previous works and our work. Obviously, the Rabi split value in this work is larger than those obtained in the traditional structures reported in [6], [23], [24], [25], [27] but less than those obtained in the complex nanostructures reported in [26], [30], [31]. Although larger Rabi split values have been obtained in [26], [30], [31], the complex structure characteristics would increase the difficulty and cost of fabrication and then hinder their further development. For example, a large Rabi splitting value of 275 meV was realized by embedding a metallic structural unit into a dielectric module to form a nested nanostructure, which involves the fine preparation of void and selective deposition of metallic material [26]. Large Rabi splitting of 220 meV or 464 meV, originating from the strong coupling of photonic BICs-cavity modes or cavity-assisted quasi-BICs-excitons, was achieved by embedding an Si or bulk WS_2 pillar pairs metasurface with symmetry broken into an FP microcavity filled with SiO_2 film [30], [31]. However, an asymmetric metasurface of air pillar pairs needs to be etched into the SiO_2 film to facilitate the insertion of the asymmetric Si or bulk WS_2 pillar pairs metasurface. Compared with these nanostructures, our structure is relatively simple and easy to be prepared by directly adhering the simple two-dimensionally periodic array of Si square nanocubes into the FP with a thin SiO_2 spacer. Therefore, the proposed silicon-based metasurface hybrid system paves an excellent platform for the acquirement of anapole-FP cavity strong coupling and large Rabi splitting.

IV. CONCLUSION

In summary, we have theoretically proposed a simple hybrid system which can be easily prepared by inserting a Si square nanocubes metasurface into a common FP nanocavity and firstly realized the strong coupling of anapole mode and FP cavity mode. The strong of anapole-FP cavity coupling induces the generation of two new hybrid energy states and a large Rabi splitting behavior with the splitting value of 192 meV. The two hybrid energy states are respectively dominated by the anapole mode and FP cavity mode and can be modified by the thickness of the SiO_2 spacer and the length of the FP nanocavity. The proposed system offers a promising avenue for realizing the strong coupling in multi-mode systems and designing high performance dielectric-based optoelectronic devices that can manipulate light-matter interactions at the nanoscale.

REFERENCES

[1] N. Muhammad, Y. Chen, C.-W. Qiu, and G. P. Wang, "Optical bound states in continuum in MoS_2-based metasurface for directional light emission," *Nano Lett.*, vol. 21, no. 2, pp. 967–972, Jan. 2021.
[2] K. F. MacDonald, Z. L. Sámson, M. I. Stockman, and N. I. Zheludev, "Ultrafast active plasmonics," *Nature Photon.*, vol. 3, no. 1, pp. 55–58, Jan. 2009.
[3] D. Sanvitto and S. Kéna-Cohen, "The road towards polaritonic devices," *Nature Mater.*, vol. 15, no. 10, pp. 1061–1073, Oct. 2016.
[4] P. Vasa and C. Lienau, "Strong light-matter interaction in quantum emitter/metal hybrid nanostructures," *ACS Photon.*, vol. 5, no. 1, pp. 2–23, Jan. 2018.
[5] J. Flick, N. Rivera, and P. Narang, "Strong light-matter coupling in quantum chemistry and quantum photonics," *Nanophotonics*, vol. 7, no. 9, pp. 1479–1501, Sep. 2018.
[6] S. You, Y. Zhang, M. Fan, S. Luo, and C. Zhou, "Strong light-matter interactions of exciton in bulk WS_2 and a toroidal dipole resonance," *Opt. Lett.*, vol. 48, no. 6, pp. 1530–1533, Mar. 2023.
[7] P. Torma and W. L. Barnes, "Strong coupling between surface plasmon polaritons and emitters: A review," *Rep. Prog. Phys.*, vol. 78, no. 1, Jan. 2015, Art. no. 013901.
[8] J. D. Plumhof, T. Stöferle, L. Mai, U. Scherf, and R. F. Mahrt, "Room-temperature Bose–Einstein condensation of cavity exciton–polaritons in a polymer," *Nature Mater.*, vol. 13, no. 3, pp. 247–252, Mar. 2014.
[9] I. Carusotto and C. Ciuti, "Quantum fluids of light," *Rev. Modern Phys.*, vol. 85, no. 1, pp. 299–366, Feb. 2013.
[10] D. E. Chang, A. S. Sørensen, E. A. Demler, and M. D. Lukin, "A single-photon transistor using nanoscale surface plasmons," *Nature Phys.*, vol. 3, no. 11, pp. 807–812, Nov. 2007.

[11] P. Bhattacharya, T. Frost, S. Deshpande, M. Z. Baten, A. Hazari, and A. Das, "Room temperature electrically injected polariton laser," *Phys. Rev. Lett.*, vol. 112, no. 23, Jun. 2014, Art. no. 236802.
[12] C. Monroe, "Quantum information processing with atoms and photons," *Nature*, vol. 416, no. 6877, pp. 238–246, Mar. 2002.
[13] T. Shibanuma, G. Grinblat, P. Albella, and S. A. Maier, "Efficient third harmonic generation from metal-dielectric hybrid nanoantennas," *Nano Lett.*, vol. 17, no. 4, pp. 2647–2651, Apr. 2017.
[14] M. Timofeeva et al., "Anapoles in free-standing III-V nanodisks enhancing second-harmonic generation," *Nano Lett.*, vol. 18, no. 6, pp. 3695–3702, Jun. 2018.
[15] J. Zhang, K. F. MacDonald, and N. I. Zheludev, "Near-infrared trapped mode magnetic resonance in an all-dielectric metamaterial," *Opt. Exp.*, vol. 21, no. 22, pp. 26721–26728, Nov. 2013.
[16] M. L. Brongersma, Y. Cui, and S. Fan, "Light management for photovoltaics using high-index nanostructures," *Nature Mater.*, vol. 13, no. 5, pp. 451–460, May 2014.
[17] A. I. Kuznetsov, A. E. Miroshnichenko, M. L. Brongersma, Y. S. Kivshar, and B. Luk'yanchuk, "Optically resonant dielectric nanostructures," *Science*, vol. 354, no. 6314, Nov. 2016, Art. no. 2472.
[18] A. E. Miroshnichenko et al., "Nonradiating anapole modes in dielectric nanoparticles," *Nature Commun.*, vol. 6, no. 1, Aug. 2015, Art. no. 8069.
[19] Y. Lu et al., " Cylindrical vector beams reveal radiationless anapole condition in a resonant state," *Opt. Exp.*, vol. 24, no. 17, pp. 19048–19062, Aug. 2016.
[20] Y. Yang, V. A. Zenin, and S. I. Bozhevolnyi, "Anapole-assisted strong field enhancement in individual all-dielectric nanostructures," *ACS Photon.*, vol. 5, no. 5, pp. 1960–1966, May 2018.
[21] T. Feng, Y. Xu, W. Zhang, and A. E. Miroshnichenko, "Ideal magnetic dipole scattering," *Phys. Rev. Lett.*, vol. 118, no. 17, Apr. 2017, Art. no. 173901.
[22] S.-D. Liu, Z.-X. Wang, W.-J. Wang, J.-D. Chen, and Z.-H. Chen, "High Q-factor with the excitation of anapole modes in dielectric split nanodisk arrays," *Opt. Exp.*, vol. 25, no. 19, pp. 22375–22387, Sep. 2017.
[23] J. Wang, W. Yang, G. Sun, Y. He, P. Ren, and Z. Yang, "Boosting anapole-exciton strong coupling in all-dielectric heterostructures," *Photon. Res.*, vol. 10, no. 7, pp. 1744–1753, Jul. 2022.
[24] S.-D. Liu, J.-L. Fan, W.-J. Wang, J.-D. Chen, and Z.-H. Chen, "Resonance coupling between molecular excitons and nonradiating anapole modes in silicon nanodisk-J-aggregate heterostructures," *ACS Photon.*, vol. 5, no. 4, pp. 1628–1639, Apr. 2018.
[25] K. Du et al., "Strong coupling between dark plasmon and anapole modes," *J. Phys. Chem. Lett.*, vol. 10, no. 16, pp. 4699–4705, Aug. 2019.
[26] W. Liu, J. Wang, H. Luo, and G. Liu, "Anapole-plasmon strong coupling induced large Rabi splitting in dielectric-metallic hybrid nanostructures," *IEEE Photon. J.*, vol. 15, no. 5, Oct. 2023, Art. no. 6500706.
[27] K. As'ham, I. Al-Ani, L. Huang, A. E. Miroshnichenko, and H. T. Hattori, "Boosting strong coupling in a hybrid WSe_2 monolayer- anapole-plasmon system," *ACS Photon.*, vol. 8, no. 2, pp. 489–496, Feb. 2021.
[28] R. Ameling and H. Giessen, "Cavity plasmonics: Large normal mode splitting of electric and magnetic particle plasmons induced by a photonic microcavity," *Nano Lett.*, vol. 10, no. 11, pp. 4394–4398, Nov. 2010.
[29] W. Li et al., "Highly efficient single-exciton strong coupling with plasmons by lowering critical interaction strength at an exceptional point," *Laser Photon. Rev.*, vol. 13, no. 1, Jan. 2019, Art. no. 1800219.
[30] P. Xie et al., "Tunable interactions of quasibound states in the continuum with cavity mode in a metasurface-microcavity hybrid," *Phys. Rev. B*, vol. 106, no. 16, Oct. 2022, Art. no. 165408.
[31] P. Xie et al., "Cavity-assisted boosting of self-hybridization between excitons and photonic bound states in the continuum in multilayers of transition metal dichalcogenides," *Phys. Rev. B*, vol. 107, no. 7, Feb. 2023, Art. no. 075415.
[32] D. G. Baranov et al., "Ultrastrong coupling between nanoparticle plasmons and cavity photons at ambient conditions," *Nature Commun.*, vol. 11, no. 1, Jun. 2020, Art. no. 2715.
[33] E. D. Palik, *Handbook of Optical Constants of Solids*. Amsterdam, The Netherlands: Elsevier, 1985.
[34] D. E. Aspnes and A. A. Studna, "Dielectric functions and optical parameters of Si, Ge, GaP, GaAs, GaSb, InP, InAs, and InSb from 1.5 to 6.0 eV," *Phys. Rev. B*, vol. 27, no. 2, pp. 985–1009, Jan. 1983.
[35] A. Vial, A.-S. Grimault, D. Macías, D. Barchiesi, and M. L. de la Chapelle, "Improved analytical fit of gold dispersion: Application to the modeling of extinction spectra with a finite-difference time-domain method," *Phys. Rev. B*, vol. 71, no. 8, Feb. 2005, Art. no. 085416.
[36] A. A. Basharin, V. Chuguevsky, N. Volsky, M. Kafesaki, and E. N. Economou, "Extremely high Q-factor metamaterials due to anapole excitation," *Phys. Rev. B*, vol. 95, no. 3, Jan. 2017, Art. no. 035104.
[37] C. Zhou, S. Li, Y. Wang, and M. Zhan, "Multiple toroidal dipole Fano resonances of asymmetric dielectric nanohole arrays," *Phys. Rev. B*, vol. 100, no. 19, Nov. 2019, Art. no. 195306.
[38] C. Zhou et al., "Optical radiation manipulation of Si-$Ge_2Sb_2Te_5$ hybrid metasurfaces," *Opt. Exp.*, vol. 28, no. 7, pp. 9690–9701, Mar. 2020.
[39] S. Zhang et al., "Coherent and incoherent damping pathways mediated by strong coupling of two-dimensional atomic crystals with metallic nanogrooves," *Phys. Rev. B*, vol. 97, no. 23, Jun. 2018, Art. no. 235401.
[40] S. Savasta, R. Saija, A. Ridolfo, O. Di Stefano, P. Denti, and F. Borghese, "Nanopolaritons: Vacuum rabi splitting with a single quantum dot in the center of a dimer nanoantenna," *ACS Nano*, vol. 4, no. 11, pp. 6369–6376, Nov. 2010.